Imaging Primary Mouse Sarcomas After Radiation Therapy Using Cathepsin-Activatable Fluorescent Imaging Agents

Citation: Cuneo, Kyle C., Jeffrey K. Mito, Melodi P. Javid, Jorge M. Ferrer, Yongbaek Kim, W. David Lee, Moungi G. Bawendi, Brian E. Brigman, and David G. Kirsch. "Imaging Primary Mouse Sarcomas After Radiation Therapy Using Cathepsin-Activatable Fluorescent Imaging Agents." International Journal of Radiation Oncology*Biology*Physics 86, no. 1 (May 2013): 136–142.

As Published: http://dx.doi.org/10.1016/j.ijrobp.2012.12.007

Publisher: Elsevier B.V.

Persistent URL: http://hdl.handle.net/1721.1/90575

Version: Final published version: final published article, as it appeared in a journal, conference proceedings, or other formally published context

International Journal of Radiation Oncology biology • physics

www.redjournal.org

Biology Contribution

Imaging Primary Mouse Sarcomas After Radiation Therapy Using Cathepsin-Activatable Fluorescent Imaging Agents

Kyle C. Cuneo, MD,* Jeffrey K. Mito, BA,† Melodi P. Javid, BS,† Jorge M. Ferrer, PhD,§ Yongbaek Kim, DVM, PhD,¶ W. David Lee, MS,‖ Moungi G. Bawendi, PhD,§ Brian E. Brigman, MD, PhD,‡ and David G. Kirsch, MD, PhD*,†

*Departments of *Radiation Oncology, †Pharmacology and Cancer Biology, and ‡Orthopedic Surgery, Duke University School of Medicine, Durham, North Carolina; §Department of Chemistry and ‖The David H. Koch Institute for Integrative Cancer Research, Massachusetts Institute of Technology, Cambridge, Massachusetts; and ¶Department of Clinical Pathology, College of Veterinary Medicine, Seoul National University, Seoul, Republic of Korea*

Received Aug 20, 2012, and in revised form Dec 3, 2012. Accepted for publication Dec 9, 2012

Summary

We examined the effect of radiation therapy (RT) on the ability of cathepsin-activated fluorescent probes to detect soft tissue sarcoma (STS) in mice. Using a primary mouse model of STS, we showed that RT does not compromise probe activation or cathepsin expression in the tumor. These results support the inclusion of patients who have undergone preoperative RT in clinical trials assessing the safety and efficacy of cathepsin-activated probes.

Purpose: Cathepsin-activated fluorescent probes can detect tumors in mice and in canine patients. We previously showed that these probes can detect microscopic residual sarcoma in the tumor bed of mice during gross total resection. Many patients with soft tissue sarcoma (STS) and other tumors undergo radiation therapy (RT) before surgery. This study assesses the effect of RT on the ability of cathepsin-activated probes to differentiate between normal and cancerous tissue.
Methods and Materials: A genetically engineered mouse model of STS was used to generate primary hind limb sarcomas that were treated with hypofractionated RT. Mice were injected intravenously with cathepsin-activated fluorescent probes, and various tissues, including the tumor, were imaged using a hand-held imaging device. Resected tumor and normal muscle samples were harvested to assess cathepsin expression by Western blot. Uptake of activated probe was analyzed by flow cytometry and confocal microscopy. Parallel in vitro studies using mouse sarcoma cells were performed.
Results: RT of primary STS in mice and mouse sarcoma cell lines caused no change in probe activation or cathepsin protease expression. Increasing radiation dose resulted in an upward trend in probe activation. Flow cytometry and immunofluorescence showed that a substantial proportion of probe-labeled cells were CD11b-positive tumor-associated immune cells.
Conclusions: In this primary murine model of STS, RT did not affect the ability of cathepsin-activated probes to differentiate between tumor and normal muscle. Cathepsin-activated probes labeled tumor cells and tumor-associated macrophages. Our results suggest that it would be feasible to include patients who have received preoperative RT in clinical studies evaluating cathepsin-activated imaging probes. © 2013 Elsevier Inc.

Reprint requests to: David G. Kirsch, MD, PhD, Departments of Radiation Oncology and Pharmacology and Cancer Biology, Duke University School of Medicine, Duke University Medical Center, Durham, NC 27710. Tel: (919) 681-8586; E-mail: david.kirsch@duke.edu

Conflict of interest: D.G.K. is a consultant as a member of the scientific advisory board for Lumicell Diagnostics, a company commercializing intraoperative imaging systems. M.G.B. and W.D.L. are founders of Lumicell Diagnostics. W.D.L. and J.M.F. are current employees of Lumicell Diagnostics. M.G.B., J.M.F., W.D.L., and D.G.K. have submitted a patent for the hand-held imaging device.

Acknowledgments—We thank Linda Griffith for helpful discussions, Tyler Jacks for providing the LSL-Kras^{G12D} mice, Martin McMahon for providing the Braf^{Ca} mice, and Anton Berns for providing the p53^{Fl} mice. This work was supported by a Damon Runyon-Rachleff Innovation Award (to D.G.K.).

Int J Radiation Oncol Biol Phys, Vol. 86, No. 1, pp. 136–142, 2013
0360-3016/$ - see front matter
http://dx.doi.org/10.1016/j.ijrobp.2012.12.007

Introduction

Soft tissue sarcoma (STS) of the extremity is commonly treated with limb-sparing surgery. In these patients, the use of adjuvant radiation therapy (RT) improves local control from approximately 66% to 90% (1-3). Compared with postoperative RT, preoperative RT is associated with increased rates of wound complications but less subcutaneous fibrosis, joint stiffness, and edema, with no significant change in local control or survival (4, 5). Therefore, preoperative RT is often used to treat patients with a high-grade STS of the extremity.

When a sarcoma is resected, a pathologist examines the resected tumor and determines whether cancer is present at the inked surgical margin. If tumor cells extend to the edge of the specimen, the margin is considered positive. A positive margin is associated with increased rates of local recurrence and reoperation (6). This method is prone to sampling error, as only a small fraction of the resected tumor is inspected. Furthermore, because the tumor bed is not examined, this method may miss skip lesions or tumor cells that have contaminated the tumor bed during surgery.

A wide field-of-view imaging system has been developed to detect microscopic residual cancer in a surgical tumor bed using a hand-held device that detects near-infrared (NIR) fluorescence (7). The imaging device has a spatial resolution of approximately 16 μm and a field of view of 9.0 × 6.6 mm, allowing one to scan a tumor bed quickly. The system has been optimized to detect NIR light, allowing for relatively increased tissue penetration. Prosense 680 and VM249 are cathepsin-activated fluorescent probes that emit a NIR signal when their peptide backbone is cleaved by cysteine proteases including cathepsins B and L. By using the hand-held imaging device, small clusters of cells that have activated VM249 or Prosense 680 can be detected in a tumor bed after surgical resection (7).

Because cathepsin proteases are preferentially expressed in STS compared to adjacent skeletal muscle (7), a cathepsin-activated fluorescent probe can provide signal contrast between the normal tissue and tumor. Preclinical studies have shown that this imaging system can detect cancer in a primary murine model of STS (7) and spontaneous cancers in canine patients (8). In the murine sarcoma model (9), the presence of NIR signal in the tumor bed correlates with microscopic residual sarcoma and local recurrence. Furthermore, the removal of tissue with residual fluorescence improves local control (7). Therefore, if this imaging technology can be successfully translated in human clinical trials, it has the potential to risk-stratify patients for local recurrence and improve outcomes.

A phase 1 clinical trial is now underway to test the safety of a cathepsin-activated fluorescent probe in patients with STS (NCT01626066). To determine whether patients receiving preoperative RT should be included in the clinical trial, we performed preclinical studies to understand the effect of radiation on the expression of cathepsin proteases, the activation of cathepsin-activated probes, and imaging of primary STS in mice.

Methods and Materials

Murine model and irradiation technique

All animal studies were performed in accordance with Institutional Animal Care and Use Committee (IACUC)-approved protocols. We used genetically engineered $Braf^{CA}$; $p53^{Fl/Fl}$ or $LSL\text{-}Kras^{G12D}$; $p53^{Fl/Fl}$ mice to generate primary STS as previously described (9). Once tumors were approximately 5 to 10 mm in greatest dimension, the mice were treated with RT to the involved hind limb. Radiation was administered in 5-Gy daily fractions to a total dose of 0, 5, 15, or 25 Gy using a single field from a XRAD 320 Biological Irradiator (Precision X-ray, North Branford, CT) at a dose rate of 2 to 2.2 Gy/min with 320 kVp photons at 12.5 mA using a 2.5-mm Al/0.1-mm Cu filter. Three orthogonal tumor dimensions were measured at regular intervals, and volumes were calculated using the following equation: Volume = π/6 (Dimension 1 * Dimension 2 * Dimension 3). Tumor volume was compared among groups using the Student *t* test.

Imaging

One week after finishing RT, mice were administered 2 nmol of VM249 (PerkinElmer, San Jose, CA) in 100 μL of phosphate-buffered saline (PBS) via tail vein injection. Six hours after injection, the mice were killed and the STS were resected. The surgical margin was inked, and muscle from the contralateral hind limb was harvested. The tumor, contralateral muscle, and tumor bed were imaged using the hand-held imaging device (Lumicell Diagnostics, Waltham, MA). Images were analyzed as previously described (7). The mean signal intensity was also calculated to determine the tumor:muscle signal ratio and the tumor:tumor bed signal ratio for each group (n=4-5). In addition, the inked tumor margin from the resected specimen was subjected to conventional histopathological analysis.

Western blot analysis

Protein isolated from tissue or cell lines was resolved on a sodium dodecyl sulfate–polyacrylamide gel electrophoresis (SDS-PAGE) gel (Biorad Laboratories, Hercules, CA), and membranes were probed with anti-Cathepsin B (sc-6493) and L (sc-6501) antibodies (Santa Cruz Biotechnology, Santa Cruz, CA). Anti-GAPDH antibody (G9545, Sigma-Aldrich, St. Louis, MO) was used as a loading control.

Imaging of individual cells placed over a simulated tumor bed

Mice bearing primary STS were injected with 2 nmol of Prosense 680 (PerkinElmer, San Jose, CA) via tail vein injection. The sarcoma was resected 24 hours later, and the tumor was homogenized and passed through a strainer to separate the tumor aggregate into individual cells. Single cells were sorted for Prosense (+) signal using flow cytometry (FACSVantage; Becton Dickinson, Franklin Lakes, NJ) and single cell suspensions were stored in PBS on ice. Within 2 hours, a simulated tumor bed was generated in recipient mice with or without prior Prosense 680 injection by exposing the gluteal muscle with a scalpel. A 50-μL quantity of the cell suspension was deposited over the exposed muscle tissue, while the area was imaged with the device. For confocal imaging (Leica SP5 Confocal Microscope; Wetzlar, Germany), normal muscle tissue was removed from tumor-free mice 24 hours after Prosense 680 injection and placed over a microscope slide, and 50 μL of the cell suspension was placed on top. Confocal images were taken at ×20 and ×63 magnification.

Immunofluorescent microscopy

Frozen sections 5 to 20 μm thick were blocked with serum and incubated with an anti-F4/80 antibody (14-4801, eBioscience, San Diego, CA) followed by an Alexa Fluor 488 labeled secondary antibody (A-21208; Invitrogen, Grand Island, NY). Nuclei were stained with 4′,6-diamidino-2-phenylindole (DAPI), and slides were imaged by confocal microscopy.

Total body irradiation and VM249 activation in normal tissues

Non-tumor-bearing *LSL-Kras^{G12D};p53$^{Fl/Fl}$* mice were treated with total body irradiation (TBI) at a dose of 720 cGy in 4 daily 180-cGy fractions using the 320 kVp x-ray source described above. One week later, irradiated and nonirradiated mice were intravenously injected with 2 nmol VM249 and sacrificed 6 hours later. Muscle, liver, small bowel, stomach, lung, kidney, and spleen were removed, washed in PBS, and imaged using the device. The mean signal intensity for each sample was obtained as described previously (7).

In vitro studies

Cells from a primary mouse STS were harvested from a *Braf^{CA};p53$^{Fl/Fl}$* mouse and cultured in Dulbecco's modified Eagle's medium (DMEM) with 10% fetal bovine serum. Sarcoma cells were plated in equal density, grown to 70% to 80% confluency, and irradiated with 0, 2, 4, or 6 Gy using the 320-kVp x-ray source at a dose rate of 2.2 Gy/min. Twenty-four hours later, VM249 was added at a concentration of 0 nmol/L, 500 nmol/L, or 1500 nmol/L. Forty-eight hours after radiation cells were harvested, washed in PBS, and resuspended with propidium iodide in PBS. Cells were analyzed and counted by flow cytometry. Scatter plots were gated and analyzed using FlowJo Software (Ashland, OR).

Results

RT does not compromise NIR signal in a murine model of STS

Braf^{CA};p53$^{Fl/Fl}$ mice were used to generate primary hind limb STS expressing *Braf^{V600E}* with *p53* deletion (7). These mice were randomized to treatment with 0, 5, 15, or 25 Gy in 5-Gy daily fractions, and tumor volume was measured every 2 to 3 days (Fig. 1A). At 7 days after completion of RT, mice treated with 15 or 25 Gy showed significant tumor growth delay compared with mice treated with a single 5-Gy fraction ($P<.05$, Fig. 1B, C). At day 5 for untreated mice and day 7 for irradiated mice, mice were injected with the cathepsin-activated fluorescent probe VM249 and sacrificed 6 hours later. The resected tumor, tumor bed, and contralateral hind limb muscle were then imaged using the hand-held device (Fig. 2A, B). The use of RT did not significantly affect the tumor:muscle signal ratio ($P<.173$, control compared to 25 Gy), but there was a trend toward a higher tumor:muscle ratio with increasing radiation dose (Fig. 2C). The tumor:tumor bed signal ratio was not significantly different for untreated mice or mice treated with 15 or 25 Gy with a histopathologically confirmed negative surgical margin (Fig. 2D).

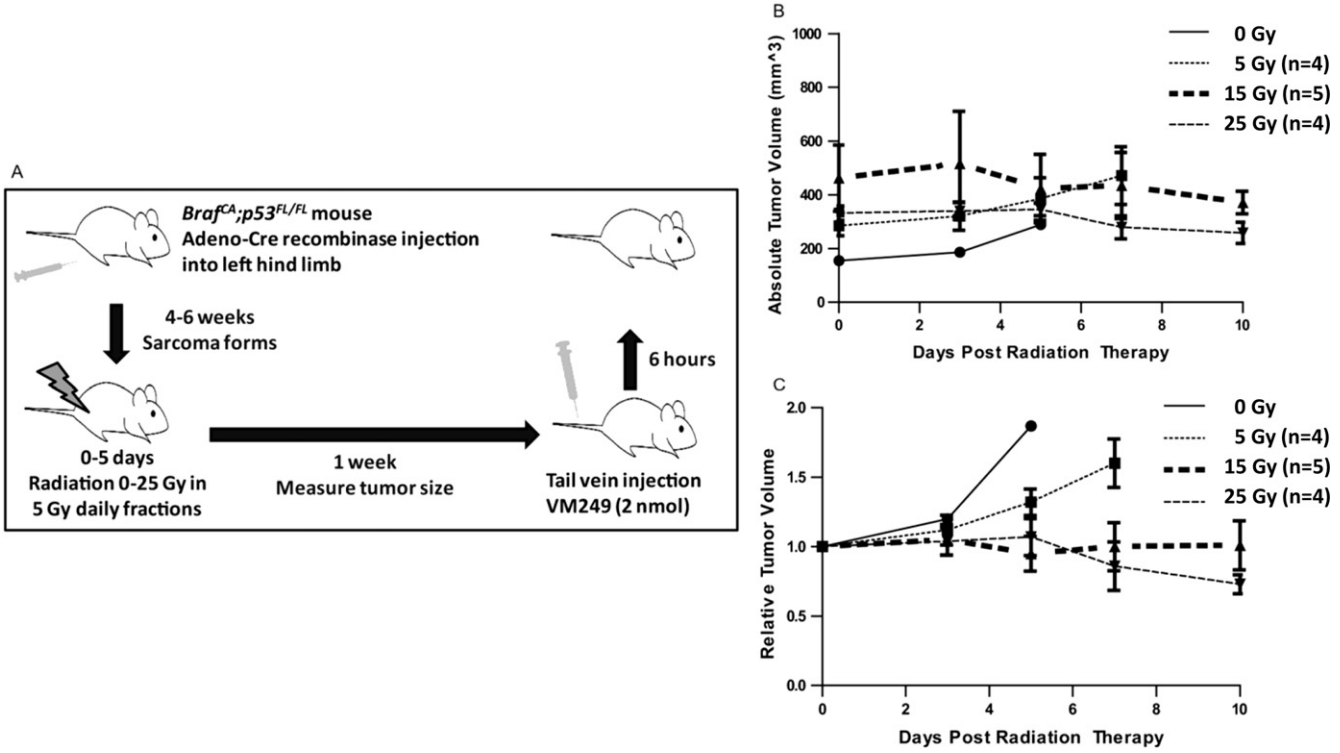

Fig. 1. Radiation therapy (RT) causes growth delay in primary soft tissue sarcoma (STS) of the hindlimb in *Braf^{CA}; p53$^{Fl/Fl}$* mice. (A) Schematic depiction of method using genetically engineered mice for generation of primary hind limb sarcomas, treatment with RT, and subsequent imaging of the tumor and related tissue. (B) Absolute change and (C) fold change in tumor volume after RT.

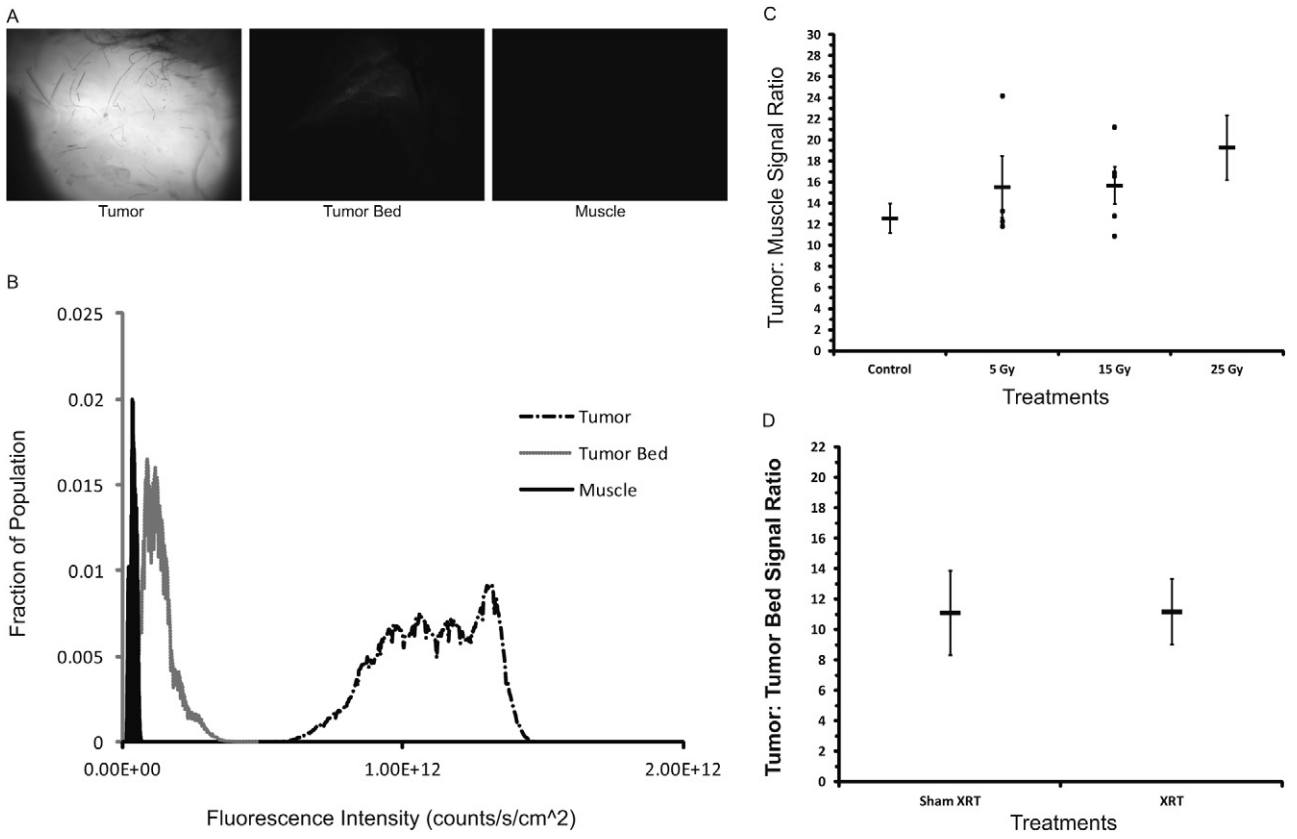

Fig. 2. Radiation therapy does not affect relative imaging signal intensity. VM249 was administered to mice from Fig. 1 and the near-infrared fluorescent signal from the imaged tissue is represented qualitatively (A) and quantitatively (B) (exposure = 5 ms). Fluorescence histograms were used to calculate the mean fluorescence intensity for each imaged tissue to determine signal ratios. (C) Tumor:normal muscle signal ratio for mice with and without RT. (D) Tumor:tumor bed signal ratio for those tumors with a histologically negative surgical margin.

Cathepsin protease expression and in vitro probe activation after RT

Western blot analysis of fresh tissue from mice with and without RT showed that Cathepsin B and L were strongly expressed in the tumor but not the muscle, and levels of expression did not change with RT (Fig. 3A).

To study the effect of RT on cathepsin expression in vitro, murine STS cells were irradiated with 0, 2, 4, or 6 Gy in a single fraction. Cells were harvested 24 hours later and analyzed by Western blot (Fig. 3B). Cathepsin B and L were strongly expressed in tumor cell lines, and expression levels did not significantly vary with increasing radiation dose.

In vitro probe activation was assessed by incubating radiation treated cells with VM249. Cells were harvested, and flow cytometry was used to quantify the percentage of viable cells labeled with VM249. RT resulted in a small (~2%/Gy), increase in labeling of cells by VM249 (Fig. 3C).

Cathepsin-activated probes label tumor parenchymal and immune cells

We examined the in vivo localization of activated probe in the tumor bed and in individual cells. Cells were harvested from a sarcoma in a mouse after injection of Prosense 680 (Fig. 4A). Prosense(+) cells were isolated and reintroduced into a simulated mouse tumor bed, where they were imaged with the hand-held device (Fig. 4B-E). Prosense(+) cells were also imaged using confocal microscopy, revealing a punctuate cytosplasmic distribution, localizing Prosense 680 within organelles, such as lysosomes (Fig. 4F).

We then studied probe activation within the native tumor environment by preparing frozen sections of primary STS from irradiated and nonirradiated mice after injection of VM249. Fluorescence microscopy of these samples demonstrates both VM249-positive tumor cells and VM249-positive F4/80-stained macrophages (Fig. 5A). VM249 activation by both cell types is maintained in mice that received RT (Fig. 5B).

In a separate experiment, STS were generated in *Rosa26*$^{YFP/YFP}$; *LSL-Kras*^{G12D}; *p53*$^{Fl/Fl}$ mice. These sarcoma cells express the yellow fluorescent protein (YFP). Mice with STS were injected with Prosense 680. Cells were isolated from the tumors of 5 mice and analyzed by flow cytometry. Of the Prosense(+) cells, 59.2 ± 6.1% were YFP(+) tumor parenchymal cells and 29.6 ± 9.1% were positive for CD11b, a marker of tumor associated macrophages (TAM) (Fig. 5D). Together, these results suggest that both sarcoma cells and TAMs are labeled by the cathepsin-activated probes.

Effects of RT on VM249 activation in organs

Non-tumor-bearing mice were treated with total body irradiation and injected with VM249. The heart, kidney, liver, lung, spleen,

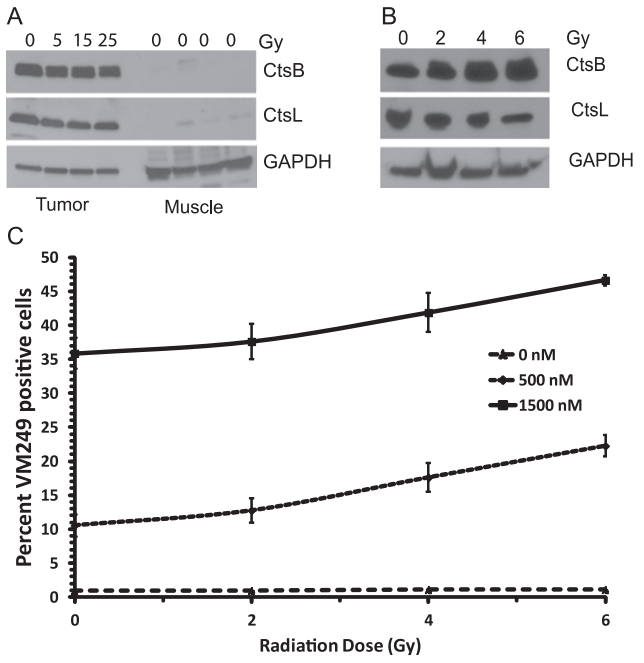

Fig. 3. Irradiation does not alter cathepsin expression or probe activation. (A) Representative cathepsin protein levels found in sarcoma and normal muscle harvested from mice that received 0, 5, 15 or 25 Gy (n=2 per radiation treatment [RT] group). (B) Cathepsin protein levels representative of 3 sarcoma cell lines treated with 0, 2, 4, or 6 Gy. (C) Flow-cytometric analysis showing the effect of RT on labeling of sarcoma cells by 500 nmol/L or 1500 nmol/L VM249.

and skeletal muscle were imaged after injection using the hand-held imaging device. RT did not significantly alter the amount of signal from VM249 in each organ imaged (Fig. 6). High levels of signal were seen in the kidney, which excretes the probe. Skeletal muscle and cardiac muscle demonstrated similar signal intensities.

Discussion

Given the high expression of cathepsin proteases in sarcomas compared with skeletal muscle, cathepsin-activated fluorescent probes are promising agents for intraoperative imaging of STS. We have shown that these probes can be used during surgery in sarcoma-bearing mice, to detect residual fluorescence in the tumor bed that correlates with residual cancer cells and local recurrence (7). Based on these results and a clinical trial testing this technology in canine patients with spontaneous tumors (8), a phase 1 clinical trial is now open to test the safety of a cathepsin-activated fluorescent probe in humans with STS or breast cancer (NCT01626066).

The utility of cathepsin-activated probes to discriminate between tumor and normal tissue has also been shown in other types of cancer. Eser et al used a murine model of pancreatic ductal adenocarcinoma to show that a cathepsin-activated NIR probe could detect low-grade lesions and could differentiate tumor from normal tissue (10). In addition, topically applied cathepsin-based probes have been used ex vivo to label human high-grade glioma specimens (11). Furthermore, 5-ALA fluorescence has been shown to complement intraoperative magnetic resonance imaging in glioma patients and to significantly improve the extent of resection (12).

There are few reports on the effect of RT on cathepsin protease expression and activity. Seo et al studied the effects of radiation on cathepsin S expression in a breast cancer model, finding that RT transiently induced cathepsin S expression (13). In the current study, cathepsins B and L were expressed at much higher levels in resected mouse sarcoma compared with skeletal muscle or tumor bed in vivo. Levels of cathepsins B and L remained constant with increasing radiation dose both in vivo and in vitro. Accordingly,

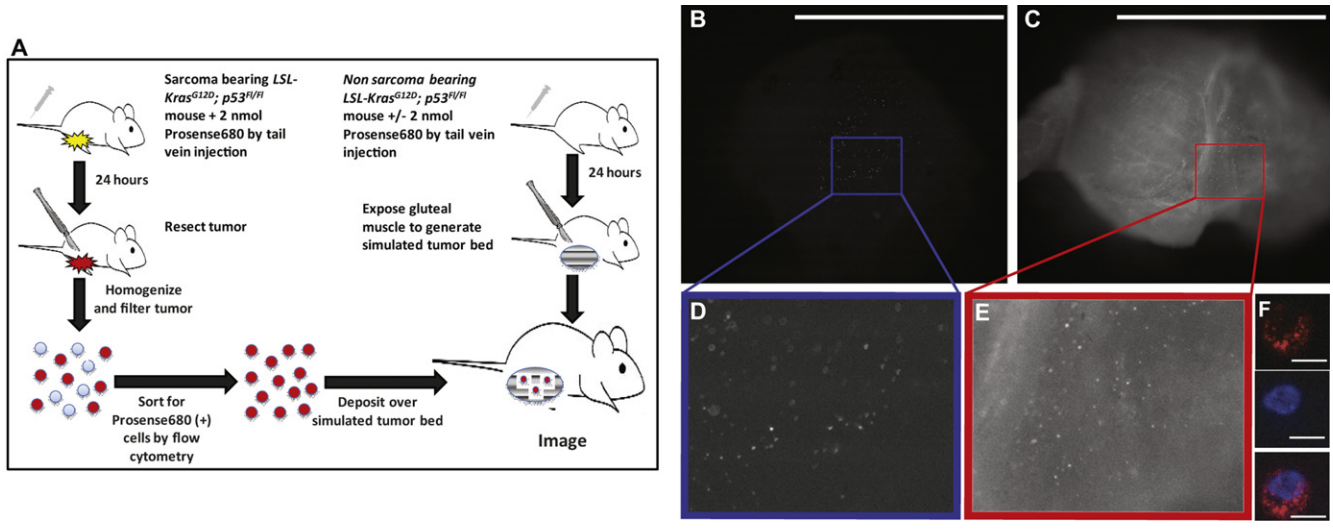

Fig. 4. Imaging individual cells transferred into simulated tumor beds in vivo. (A) Cells were obtained by flow cytometry from a sarcoma-bearing mouse 24 hours after Prosense 680 injection. Individual Prosense (+) cells from the sarcoma were detected by the hand-held imaging device when placed in a simulated tumor bed from a mouse not injected (B) and injected (C) with Prosense 680. (F) Prosense signal was confirmed to originate from individual cells by confocal microscopy in the Prosense channel (top, red) and nuclear Hoechst stain (middle, blue), which were merged together (bottom). Insets in B and C show a ×2.5 magnification of the highlighted area (D, E). Scale bars = 5 mm for B and C, and 10 μm for F.

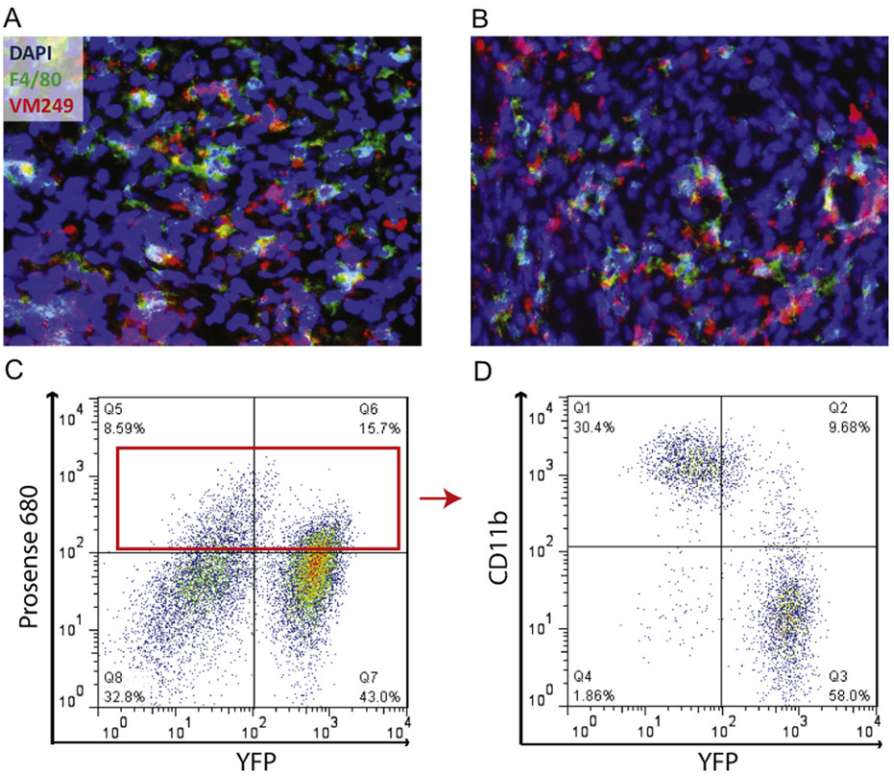

Fig. 5. Probe activation and the tumor microenvironment. (A) Untreated mice or (B) mice treated with 5 Gy were injected with VM249 7 days after completion of RT. Tumors were harvested 6 hours after probe injection, and unfixed tumor frozen sections were stained with the macrophage marker F4/80 and nuclear stain DAPI (images are representative of 4 mice per treatment group). (C) Flow cytometry plots are representative of 5 mice, showing tumor cells from sarcoma bearing *Rosa26*$^{YFP/YFP}$; *LSL-Kras*^{G12D}; *p53*$^{Fl/Fl}$ mice that were injected with Prosense 680 24 hours before tumor harvest. (D) Staining for CD11b was used to analyze Prosense 680 labeled cells for tumor associated immune cells.

probe activation did not change significantly with RT, indicating that cathepsin activity is not modulated by radiation.

Tumor associated macrophages play an important role in the activation of cathepsin-activated probes in this system, as approximately 30% of the cells that activated cathepsin-based probes were CD11b(+). Immunofluorescence studies showed RT independent co-localization of probe to both tumor parenchymal and immune cells. These data suggest that RT does not reduce probe activation by cathepsin proteases expressed by tumor parenchyma or immune cells.

There are several limitations to our preoperative radiation murine model. The National Comprehensive Cancer Network (NCCN) recommends treatment in 2-Gy fractions to 50 Gy for patients with STS receiving neoadjuvant RT (14). In the current study, mice were treated with 5-Gy fractions from 0 to 25 Gy, which is the equivalent 2-Gy dose (EQD_2) of 40 Gy, assuming an α/β ratio of 3. In addition, there is typically a 1-month break after finishing RT before surgery. In this study, murine sarcomas were resected after 1 week because of rapid tumor growth. Finally, this murine sarcoma model is most similar to undifferentiated pleomorphic sarcoma compared with other STS subtypes (15), and the treatment effect as assessed by histology appeared to be modest with this dose and schedule of RT. It is possible that for some subtypes of STS, such as myxoid liposarcoma, which are particularly responsive to radiation (16), the effect on cathepsin-activated probes would be more substantial.

Despite these limitations, the imaging system was effective at differentiating tumor from muscle after RT, as neither the tumor:muscle nor the tumor:tumor bed signal ratios were compromised. Furthermore, TBI did not significantly alter the signal from VM249 in several types of normal tissue. In vitro, radiation resulted in a small increase in VM249 activation in tumor cells. Taken together, these findings indicate that the use of

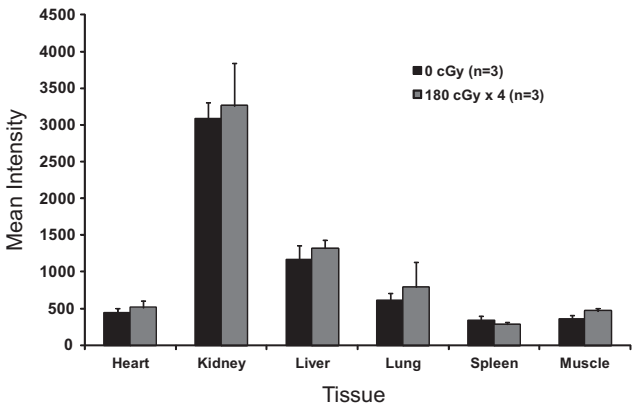

Fig. 6. Background probe activation in different tissues is not affected by total body irradiation. Mice without tumors were treated with TBI to 0 Gy or 7.2 Gy in 180-cGy daily fractions and injected with VM249 1 week later. The mice were killed 6 hours after injection, at which time individual organs were removed, washed in phosphate-buffered saline, and imaged using the hand-held device.

preoperative RT does not impair the ability of cathepsin-activated imaging probes to preferentially label sarcomas compared with normal muscle. Therefore, this study supports the inclusion of patients treated with preoperative RT in the phase 1 clinical trial testing this technology.

References

1. Yang JC, Chang AE, Baker AR, et al. Randomized prospective study of the benefit of adjuvant radiation therapy in the treatment of soft tissue sarcomas of the extremity. *J Clin Oncol* 1998;16:197-203.
2. Pisters PW, Harrison LB, Leung DH, et al. Long-term results of a prospective randomized trial of adjuvant brachytherapy in soft tissue sarcoma. *J Clin Oncol* 1996;14:859-868.
3. Pisters PW, Leung DH, Woodruff J, et al. Analysis of prognostic factors in 1,041 patients with localized soft tissue sarcomas of the extremities. *J Clin Oncol* 1996;14:1679-1689.
4. O'Sullivan B, Davis AM, Turcotte R, et al. Preoperative versus postoperative radiotherapy in soft-tissue sarcoma of the limbs: a randomised trial. *Lancet* 2002;359:2235-2241.
5. Davis AM, O'Sullivan B, Turcotte R, et al. Late radiation morbidity following randomization to preoperative versus postoperative radiotherapy in extremity soft tissue sarcoma. *Radiother Oncol* 2005; 75:48-53.
6. Lewis JJ, Leung D, Casper ES, et al. Multifactorial analysis of long-term follow-up (more than 5 years) of primary extremity sarcoma. *Arch Surg* 1999;134:190-194.
7. Mito JK, Ferrer JM, Brigman BE, et al. Intraoperative detection and removal of microscopic residual sarcoma using wide-field imaging. *Cancer* 2012;118:5320-5330.
8. Eward WC, Mito JK, Eward CA, et al. A novel imaging system permits real-time in vivo tumor bed assessment after resection of naturally occurring sarcomas in dogs. *Clin Orthop Relat Res* 2012 Sep 13 [epub ahead of print Sep 13 2012].
9. Kirsch DG, Dinulescu DM, Miller JB, et al. A spatially and temporally restricted mouse model of soft tissue sarcoma. *Nat Med* 2007;13:992-997.
10. Eser S, Messer M, Eser P, et al. In vivo diagnosis of murine pancreatic intraepithelial neoplasia and early-stage pancreatic cancer by molecular imaging. *Proc Natl Acad Sci U S A* 2011;08:9945-9950.
11. Cutter JL, Cohen NT, Wan J, et al. Topical application of activity-based probes for visualization of brain tumor tissue. *PLoS One* 2012;7(3):e33060.
12. Eyupoglu IY, Hore N, Savaskan NE, et al. Improving the extent of malignant glioma resection by dual intraoperative visualization approach. *PLoS One* 2012;7(9):e44885.
13. Seo HR, Bae S, Lee YS. Radiation-induced cathepsin S is involved in radioresistance. *Int Jf Cancer* 2009;124:1794-1801.
14. NCCN Guidelines: Soft Tissue Sarcoma. 2012. www.nccn.org. Accessed May 5, 2012.
15. Mito JK, Riedel RF, Dodd L, et al. Cross species genomic analysis identifies a mouse model as undifferentiated pleomorphic sarcoma/malignant fibrous histiocytoma. *PLoS One* 2009;4:e8075.
16. Chung PW, Deheshi BM, Ferguson PC, et al. Radiosensitivity translates into excellent local control in extremity myxoid liposarcoma: a comparison with other soft tissue sarcomas. *Cancer* 2009;115:3254-3261.